

---

# Numerical Zoom and the Schwarz Algorithm

Frédéric Hecht<sup>1</sup>, Alexei Lozinski<sup>2</sup>, and Olivier Pironneau<sup>1</sup>

<sup>1</sup> Laboratoire Jacques-Louis Lions - Université Pierre et Marie Curie  
Frederic.Hecht@upmc.fr and Olivier.Pironneau@upmc.fr

<sup>2</sup> Institut de Mathématiques de Toulouse, Université Paul Sabatier  
alexei.lozinski@math.univ-toulouse.fr

**Summary.** We investigate Schwarz' domain decomposition algorithm as a tool for numerical zoom and compare it with the Subspace Correction Method. Quadrature error is investigated and the convergence of Schwarz' algorithm is sketched for non matching grids. The methods are also compared numerically.

## 1 Introduction

Often enough engineers do a coarse calculation and then a finer one on a subset (zoom)  $\Lambda$  of the whole domain  $\Omega$ . We wish here to justify this approach, i.e. to study convergence and errors when the strategy is made into a loop. Obviously one zoom calculation is not enough, unless the problem is nonlinear or time dependent and the iterations for the zoom are seen as part of the nonlinear or time loop.

So the situation is as follows: a coarse calculation is done in  $\Omega$ , then another one in a zoom  $\Lambda \subset \Omega$ . The question then is how to set properly the problem in  $\Lambda$  and how to feed in intelligently its solution into the coarse solver to correct it?

### Chimera

The chimera method proposed by Steger[11], originally for nonlinear time dependent problems, digs a hole  $D$  in the coarse domain strictly inside the zoom region  $\Lambda$ . For example, to compute the hydrostatic pressure  $u$  of a porous media flow given its value on  $\partial\Omega$  and governed by Darcy's law with porosity  $K$ ,

$$u - g \in H_0^1(\Omega) : -\nabla \cdot (K\nabla u) = f \quad \text{in } \Omega \quad (1)$$

one chooses a sub-domain  $D$  strictly inside  $\Lambda$  and loops on  $n$  on the two problems:

Chimera is identical to Schwarz' algorithm for domain decomposition, but the Computational Fluid Dynamic community uses this terminology. In our numerical experiments in the present paper, the hole  $D$  will always be chosen as a union of several triangles from the coarse mesh on  $\Omega$  and  $U^n|_{\partial D} = u^{n-1}|_{\partial D}$  will be approximated

**Require:** An initial guess is needed, for instance  $u_H^0 = g_H$

1: **for**  $n = 1 \dots N$  **do**

2: Solve

$$-\nabla \cdot (K \nabla U^n) = f \text{ in } \Omega \setminus D, \quad (U^n - g)|_{\partial \Omega} = 0, \quad U^n|_{\partial D} = u^{n-1}|_{\partial D}, \quad (2)$$

3: Solve

$$-\nabla \cdot (K \nabla u^n) = f \text{ in } \Lambda, \quad u^n = U^n \text{ on } \partial \Lambda. \quad (3)$$

4: **end for**

#### Algorithm 2: Chimera

by taking the values of  $u^{n-1}$  at the coarse grid vertices of  $\partial D$ . Although this seems to work fine in most cases, the convergence in the natural energy norm is an open problem, as well as the precision because of the unavoidable interpolation of  $U^n$  on  $\partial \Lambda$  when  $\Lambda$  is not made of elements of the triangulation of  $\Omega$ . The theoretical analysis of this method will be done here in the maximum norm. Note that an alternative way to impose  $U^n|_{\partial D} = u^{n-1}|_{\partial D}$  (even with an arbitrary form of  $\partial D$ ) would be to use boundary penalty on  $\partial D$  or volumic penalty on  $D$ . However, such implementations do not perform well in practice as reported in [9].

### Hilbert Space Decomposition Method

An alternative idea introduced in [12] and studied in [2, 3] amounts, formally speaking, to finding a subspace correction  $u$  to the coarse solution, i.e.

find  $U, u$  with  $U - g \in H_0^1(\Omega), u \in H_0^1(\Lambda)$  and

$$\int_{\Omega} (K \nabla(U + u) \cdot \nabla(W + w) - f(W + w)) = 0 \quad \forall W \in H_0^1(\Omega), w \in H_0^1(\Lambda) \quad (4)$$

This equation is easy to discretize, with  $u_H \approx U$ ,  $u_h \approx u$ , and a simple iterative scheme such as Algorithm 3. We use there the following notations:  $V_H$  and  $V_h$  are finite element spaces on some regular triangulations  $\mathcal{T}_H$  and  $\mathcal{T}_h$  of  $\Omega$  and  $\Lambda$  respectively;  $V_{0H} = V_H \cap H_0^1(\Omega)$ ;  $V_{gH}$  is the subspace of  $V_H$  consisting of functions equal to  $g_H$  on  $\partial \Omega$ , and  $V_{0h} = V_h \cap H_0^1(\Lambda)$ .

When  $\Lambda \subset \Omega$ , Algorithm 3 is also known as the *patch iterator* [7]. The solution  $u_{Hh} = \lim_{n \rightarrow \infty} (u_H^n + u_h^n)$  thus obtained satisfies the following error estimate even if the two meshes  $\Omega_H$  and  $\Lambda_h$  do not match:

$$\|u - u_{Hh}\|_{H^1(\Omega)} \leq C(H^r \|u\|_{H^q(\Omega \setminus \bar{\Lambda})} + h^s \|u\|_{H^q(\Lambda)}), \quad (7)$$

where  $r$  and  $s$  are the maximal degrees of the polynomials used in the construction of  $V_H$  and  $V_h$  respectively and  $q = \max(r, s) + 1$ .

**Require:** an initial guess  $u_h^0 \in V_{0h}$  is needed.

- 1: **for**  $n = 1 \dots N$  **do**
- 2: Find  $u_H^n \in V_{gH}$  by

$$\int_{\Omega} K \nabla u_H^n \cdot \nabla w_H = \int_{\Omega} f w_H - \int_{\Omega} K \nabla u_h^{n-1} \cdot \nabla w_H \quad \forall w_H \in V_{0H} \quad (5)$$

- 3: Find  $u_h^n \in V_{0h}$  by

$$\int_{\Lambda} K \nabla u_h^n \cdot \nabla w_h = \int_{\Lambda} f w_h - \int_{\Lambda} K \nabla u_H^n \cdot \nabla w_h \quad \forall w_h \in V_{0h} \quad (6)$$

- 4: **end for**

Algorithm 3: Hilbert Space Decomposition

### Harmonic Patch Iterator

The drawback of Hilbert Decomposition method is that its convergence can be very slow when the triangulations  $\mathcal{T}_H, \mathcal{T}_h$  are not nested. The method needs to be improved; this is the object of Algorithm 4, the Harmonic patch method of [8]. To write it down, we need the following (normally low dimensional) subspace of  $V_H$ :

$$V_H^0 = \{v_H \in V_H : \text{supp } v_H \subset \Lambda\}.$$

**Require:** an initial guess  $u_h^0 \in V_{0h}$ .

- 1: **for**  $n = 1 \dots N$  **do**
- 2: Find  $\lambda_H^n \in V_H^0$  such that

$$\int_{\Omega} K \nabla \lambda_H^n \cdot \nabla \mu_H = \int_{\Omega} f \mu_H - \int_{\Omega} K \nabla u_h^{n-1} \cdot \nabla \mu_H \quad \forall \mu_H \in V_H^0 \quad (8)$$

- 3: Find  $u_H^n \in V_{gH}$  by

$$\int_{\Omega} K \nabla u_H^n \cdot \nabla w_H = \int_{\Omega} f w_H - \int_{\Omega} K \nabla u_h^{n-1} \cdot \nabla w_H - \int_{\Omega} K \nabla \lambda_H^n \cdot \nabla w_H \quad \forall w_H \in V_{0H} \quad (9)$$

- 4: Find  $u_h^n \in V_{0h}$  by

$$\int_{\Lambda} K \nabla u_h^n \cdot \nabla w_h = \int_{\Lambda} f w_h - \int_{\Lambda} K \nabla u_H^n \cdot \nabla w_h = 0 \quad \forall w_h \in V_{0h} \quad (10)$$

- 5: **end for**

Algorithm 4: Harmonic patch iterator

The new variable  $\lambda_H^n$  is merely auxiliary, and the solution is recovered as  $u_{Hh} = \lim_{n \rightarrow \infty} (u_H^n + u_h^n)$  exactly as in the case of Algorithm 3. In fact these two algorithms are identical in the case of nested triangulations, in the sense that  $u_H^n + u_h^n$  is then rigorously the same in Algorithms 3 and 4 for all  $n \geq 1$  although each  $u_H^n$  and  $u_h^n$  may differ from one algorithm to another. In general,  $u_{Hh}$  obtained by the Harmonic

Patch Iterator can be slightly different from the limiting solution of Algorithm 3 but it still satisfies the *a priori* error estimate (7). The additional problem for  $\lambda_H^n$  is normally very cheap to solve permitting a great increase of the convergence rate in comparison with Algorithm 3 as confirmed by the numerical experiments in [8].

### One Way Schwarz

If (as will be done in this paper) in order to facilitate the evaluation of  $\int_{\Lambda} K \nabla u_H^n \cdot \nabla w_h$  in (6), one approximates  $u_H^n$  there by its interpolation  $\gamma_h u_H^n$  on  $\mathcal{T}_h$ , then the resulting problem for  $u_h^n$  can be simplified. Namely, one introduces in each iteration the new unknown  $w_h^n \in V_h$  as  $w_h^n = \gamma_h u_H^n|_{\Lambda} + u_h^n$  so that  $w_h^n$  solves the same problem (3) as the fine correction  $u^n$  in the Schwarz algorithm 2. One can rewrite then Algorithm 3 in terms of  $u_H^n$  and  $w_h^n$  (without distinguishing between  $\gamma_h u_H^{n-1}$  and  $u_H^{n-1}$  in the coarse correction step) and this leads to the ‘‘One way Schwarz’’ algorithm 5 proposed in [9]. Note that the successive approximations  $u_{Hh}^n$  to  $u$  should be defined here as  $u_{Hh}^n = \{w_h^n \text{ in } \Lambda, u_H^n \text{ outside } \Lambda\}$  just as in the Schwarz algorithm.

**Require:** 2 initial guesses  $u_H^0 \in V_{gH}$  and  $w_h^0 \in V_h$  such that  $w_h^0 = \gamma_h u_H^0$  on  $\partial\Lambda$ .

1: **for**  $n = 1 \dots N$  **do**

2: Find  $u_H^n \in V_{gH}$  by

$$\int_{\Omega} K \nabla u_H^n \cdot \nabla v_H = \int_{\Omega} f v_H + \int_{\Lambda} K \nabla (u_H^{n-1} - w_h^{n-1}) \cdot \nabla v_H \quad \forall v_H \in V_{0H} \quad (11)$$

3: Find  $w_h^n \in V_h$  with

$$\int_{\Lambda_h} K \nabla w_h^n \cdot \nabla v_h = \int_{\Lambda_h} f v_h \quad \forall v_h \in V_{0h}, \quad w_h^n = \gamma_h u_H^n \text{ on } \partial\Lambda \quad (12)$$

4: **end for**

#### Algorithm 5: One way Schwarz

The equivalence of Algorithms 3–5 is readily seen in the nested case. In a general situation, the relations between them are rather complicated because of interpolations from one mesh to another. One can see though that our last algorithm is closer to the harmonic version 4, but its performance in practice is situated between those of Algorithms 3 and 4, see [9].

As the subspace correction methods such as Algorithms 3–5 can in principle be prone to instabilities due to the quadrature errors, we wish here to study the Chimera idea more carefully. The convergence of Algorithm 2 and an error estimate for it will be proved in the maximum norm under some natural hypotheses. It will be also numerically compared with Algorithms 3–4.

## 2 Convergence of Schwarz' Algorithm on Arbitrary Non-Matching Meshes

Convergence of multidomain approximations with overlap of arbitrary finite element meshes is known only in the case of the Mortar method [1]. Convergence of Schwarz' algorithm on arbitrary uniform meshes has been shown by Cai et al. [4] only for finite difference discretization. Their proof relies on the maximum principle and the exponential decay of the solution of elliptic pdes far from the boundaries. The same ideas are used here for triangular first order finite elements.

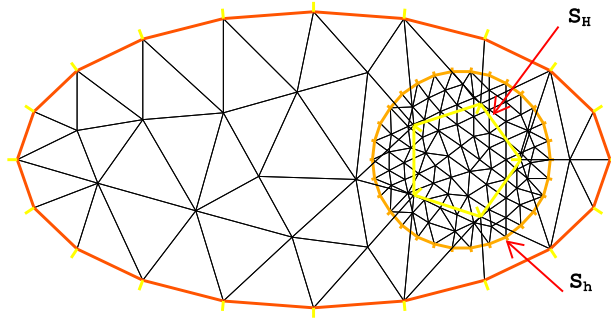


Fig. 1. Triangulations showing  $\Omega_H$  outside  $S_H$  and  $\Omega_h$  inside  $S_h$ .

To solve

$$-\Delta u = f \text{ in } \Omega \quad \text{with} \quad u = g \text{ on } \Gamma = \partial\Omega, \quad (13)$$

we choose two subsets of  $\Omega$ ,  $\Omega_H$  and  $\Omega_h$  and two triangulations  $\mathcal{T}_H$  of  $\Omega_H$ ,  $\mathcal{T}_h$  of  $\Omega_h$ , such that

$$\Omega_H \cup \Omega_h = \Omega, \quad \partial\Omega_h \subset \Omega_H, \quad \partial\Omega_h \cap \Gamma = \emptyset, \quad \partial\Omega_H \setminus \Gamma \subset \Omega_h.$$

As in Fig. 1 we denote by  $S_h$  the boundary of  $\Omega_h$  and by  $S_H$  the part of the boundary of  $\Omega_H$  different from  $\Gamma_H$ . Next, let

$$V_H = \{v \in C^0(\Omega_H) : v|_K \in P^1, \forall K \in \mathcal{T}_H\}, \quad V_{0H} = \{v \in V_H : v|_{\partial\Omega_H} = 0\},$$

and similarly with  $h$ . Starting from  $u_H^0 = 0$ ,  $u_h^0 = 0$ , the discrete Schwarz algorithm (same as Chimera Algorithm 2) finds  $u_H^m \in V_H$  and  $u_h^m \in V_h$  such that  $\forall w_H \in V_{0H}$ ,  $\forall w_h \in V_{0h}$ :

$$\begin{aligned} a_H(u_H^m, w_H) &= (f, w_H), & u_H^m|_{S_H} &= \gamma_H u_h^{m-1}, & u_H^m|_{\Gamma_H} &= g_H \\ a_h(u_h^m, w_h) &= (f, w_h), & u_h^m|_{S_h} &= \gamma_h u_H^m, \end{aligned} \quad (14)$$

where  $a_{H,h}(u, v) = \int_{\Omega_{H,h}} \nabla u \cdot \nabla v$  and  $\gamma_H$  (resp  $\gamma_h$ ) is the interpolation operator on  $V_H$  (resp  $V_h$ ).

**Hypothesis 1** Assume that the maximum principle holds for each system in (14) independently. Further assume that the solution  $v_H \in V_H$  of

$$a_H(v_H, w_H) = 0 \quad \forall w_H \in V_{0H}, \quad v_H|_{S_H} = 1, \quad v_H|_{\Gamma_H} = 0, \quad (15)$$

satisfies  $|v_H|_{\infty, S_h} := \lambda < 1$ .

*Remark 1.* Notice that the maximum principle is known to be true when all the angles of the triangulation are acute [5]. The strict maximum principle of the hypothesis could be checked numerically, a priori. Error estimates in maximum norm of order  $h^2 \log \frac{1}{h}$  with respect to the mesh edge size  $h$  for linear elements have been obtained by Schatz et al. [13].

**Proposition 1.** *Assume Hypothesis 1 to be satisfied. Then the discrete Schwarz algorithm (14) converges to the unique solution  $(u_h^*, u_H^*) \in V_h \times V_H$  of the following system:*

$$\begin{aligned} a_H(u_H^*, w_H) &= (f, w_H) \quad \forall w_H \in V_{0H}, \quad u_H^*|_{S_H} = \gamma_H u_h^*, \quad u_H^*|_{\Gamma_H} = g_H \\ a_h(u_h^*, w_h) &= (f, w_h) \quad \forall w_h \in V_{0h}, \quad u_h^*|_{S_h} = \gamma_h u_H^*. \end{aligned} \quad (16)$$

*Proof.* By the maximum principle and the fact that  $\gamma_H$  and  $\gamma_h$  decrease the  $L^\infty$  norms, problems of the type: find  $v_H \in V_H$ ,  $v_h \in V_h$

$$\begin{aligned} a_H(v_H, w_H) &= 0 \quad \forall w_H \in V_{0H}, \quad v_H|_{S_H} = \gamma_H u_h, \quad v_H^{m+1}|_{\Gamma_H} = 0 \\ a_h(v_h, w_h) &= 0 \quad \forall w_h \in V_{0h}, \quad v_h^{m+1}|_{S_h} = \gamma_h v_H, \end{aligned} \quad (17)$$

satisfy

$$\|v_H\|_\infty \leq \|u_h\|_{\infty, S_H}, \quad \|v_h\|_\infty \leq \|v_H\|_{\infty, S_h}. \quad (18)$$

Combining this with the estimate on the solution of (15) we obtain

$$\|v_h\|_\infty \leq \|v_H\|_{\infty, S_h} \leq \lambda \|v_H\|_\infty \leq \lambda \|u_h\|_\infty. \quad (19)$$

Consider now the mapping  $T : V_h \rightarrow V_h$  that maps any  $u_h^{m-1}$  in (14) to  $u_h^m$ . Since  $T$  is affine, estimate (19) the problem (17) proves that  $T$  is a contraction in the  $L^\infty(\Omega_h)$  norm. By Banach contraction theorem we have then that the iterative process  $u_h^m = T u_h^{m-1}$  converges to the unique fixed point  $u_h^*$  of  $T$ . In other words,  $u_h^m$  given by (14) converges to  $u_h^*$  in (16), which entails the convergence of  $u_H^m$  to  $u_H^*$ .

**Proposition 2.** *Assume Hypothesis 1 to be satisfied. Then  $(u_h^*, u_H^*)$  in (16) solves approximately (13) with optimal  $L^\infty$  error. More precisely, we have*

$$\begin{aligned} \max(\|u_H^* - u\|_{\infty, \Omega_H}, \|u_h^* - u\|_{\infty, \Omega_h}) &\leq \\ &C \left( H^2 \log \frac{1}{H} \|u\|_{H^{2,\infty}(\Omega_H)} + h^2 \log \frac{1}{h} \|u\|_{H^{2,\infty}(\Omega_h)} \right), \end{aligned} \quad (20)$$

with a constant  $C$  depending only on the domains  $\Omega_H$  and  $\Omega_h$ .

*Proof.* Solution  $u$  to problem (13) satisfies  $u|_\Gamma = g$  and

$$\begin{aligned} a_H(u, w) &= (f, w) \quad \forall w \in H_0^1(\Omega_H), & u &= \gamma_H u + (u - \gamma_H u) \quad \text{on } S_H, \\ a_h(u, w) &= (f, w) \quad \forall w \in H_0^1(\Omega_h), & u &= \gamma_h u + (u - \gamma_h u) \quad \text{on } S_h. \end{aligned} \quad (21)$$

Let  $e = u_H^* - u$  and  $\varepsilon = u_h^* - u$ . Setting  $w = w_H$  in the first equation and  $w = w_h$  in the second, we have

$$\begin{aligned} a_H(e, w_H) &= 0 \quad \forall w_H \in V_{0H}, & e &= \gamma_H \varepsilon - (u - \gamma_H u) \quad \text{on } S_H, & e|_\Gamma &= g_H - g \\ a_h(\varepsilon, w_h) &= 0 \quad \forall w_h \in V_{0h}, & \varepsilon &= \gamma_h e - (u - \gamma_h u) \quad \text{on } S_h. \end{aligned} \quad (22)$$

Let  $\Pi_H u \in V_H$  and  $\Pi_h u \in V_h$  be the solutions of

$$\begin{aligned} a_H(\Pi_H u, w_H) &= a_H(u, w_H) \quad \forall w_H \in V_{0H}, & \Pi_H u &= \gamma_H u \quad \text{on } S_H, & \Pi_H u|_\Gamma &= g_H \\ a_h(\Pi_h u, w_h) &= a_h(u, w_h) \quad \forall w_h \in V_{0h}, & \Pi_h u &= \gamma_h u \quad \text{on } S_h. \end{aligned} \quad (23)$$

By [13], we have

$$\begin{aligned} \|\Pi_H u - u\|_{\infty, \Omega_H} &\leq H^2 \log \frac{1}{H} \|u\|_{H^{2,\infty}(\Omega_H)}, \\ \|\Pi_h u - u\|_{\infty, \Omega_h} &\leq h^2 \log \frac{1}{h} \|u\|_{H^{2,\infty}(\Omega_h)}. \end{aligned} \quad (24)$$

Finally let

$$\varepsilon_H = u_H - \Pi_H u = e + u - \Pi_H u, \quad \varepsilon_h = u_h - \Pi_h u = \varepsilon + u - \Pi_h u.$$

Then  $\varepsilon_H \in V_H$ ,  $\varepsilon_h \in V_h$  and

$$\begin{aligned} a_H(\varepsilon_H, w_H) &= 0 \quad \forall w_H \in V_{0H}, & \varepsilon_H &= \gamma_H(\varepsilon_h + \Pi_h u - u) \quad \text{on } S_H, & \varepsilon_H|_\Gamma &= 0 \\ a_h(\varepsilon_h, w_h) &= 0 \quad \forall w_h \in V_{0h}, & \varepsilon_h &= \gamma_h(\varepsilon_H + \Pi_H u - u) \quad \text{on } S_h. \end{aligned} \quad (25)$$

The maximum principle (like in (18) and (19)) again yields

$$\|\varepsilon_H\|_\infty \leq \|\Pi_h u - u\|_{\infty, S_H} + \|\varepsilon_h\|_{\infty, S_H}, \quad (26)$$

$$\|\varepsilon_h\|_\infty \leq \|\Pi_H u - u\|_{\infty, S_h} + \|\varepsilon_H\|_{\infty, S_h}, \quad (27)$$

$$\|\varepsilon_H\|_{\infty, S_h} \leq \lambda \|\varepsilon_H\|_\infty. \quad (28)$$

Therefore

$$\max(\|\varepsilon_h\|_\infty, \|\varepsilon_H\|_\infty) \leq \frac{1}{1-\lambda} (\|\Pi_H u - u\|_{\infty, \Omega_H} + \|\Pi_h u - u\|_{\infty, \Omega_h}). \quad (29)$$

Combining it with (24) and the triangle inequality we obtain the desired result.

### Numerical Tests

We have tested numerically the Schwarz algorithm for the problem  $u - \Delta u = xy$ ,  $u|_{\partial\Omega} = xy$  with the solution  $u = xy$  and the geometry shown in Fig. 2a. All the computations were done using the integrated environment freefem++ [10]. Convergence of the Schwarz iterations is illustrated in Fig. 2b. The results show that the convergence is linear and  $\|u_h^{m+1} - u_h^*\|_0 / \|u_h^m - u_h^*\|_0 \rightarrow 0.67$  while the constant  $\lambda$  in the Hypothesis 1 is  $\lambda = 0.75$ . When the two meshes are refined by the factor of 2 or 4, these figures do not change much.

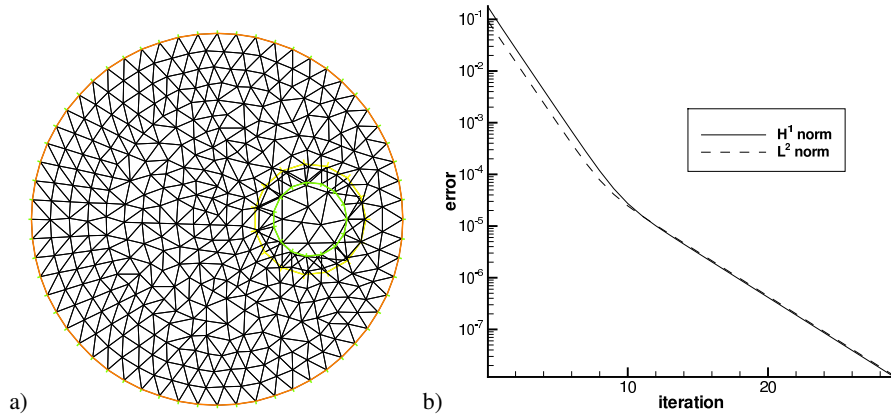


**Fig. 2.** a) The geometry of  $\Omega_H, \Omega_h$  and the meshes M1; b) Convergence on Schwarz iterations, error with respect to the final discrete solution.

Let us now look at the behavior of the converged Schwarz solution with respect to the mesh refinement. Figure 3c shows it for the mesh M1 as in Fig. 2a, and the error is plotted in Fig. 3d. Table 1 reports the error on three pairs of meshes, namely M1, their twofold refinement M2 and the 4-times refinement M4. We observe the optimal convergence rates

	$H^1$	$L^2$	$L^\infty$
M1	$7.2 \cdot 10^{-3}$	$1.4 \cdot 10^{-3}$	$4.0 \cdot 10^{-3}$
M2	$3.6 \cdot 10^{-3}$	$2.9 \cdot 10^{-4}$	$1.2 \cdot 10^{-3}$
M3	$1.6 \cdot 10^{-3}$	$9.8 \cdot 10^{-5}$	$3.8 \cdot 10^{-4}$

**Table 1.** The relative error in  $H^1, L^2$  and  $L^\infty$  norms for the approximated solutions obtained by Schwarz algorithm on meshes M1–M3.

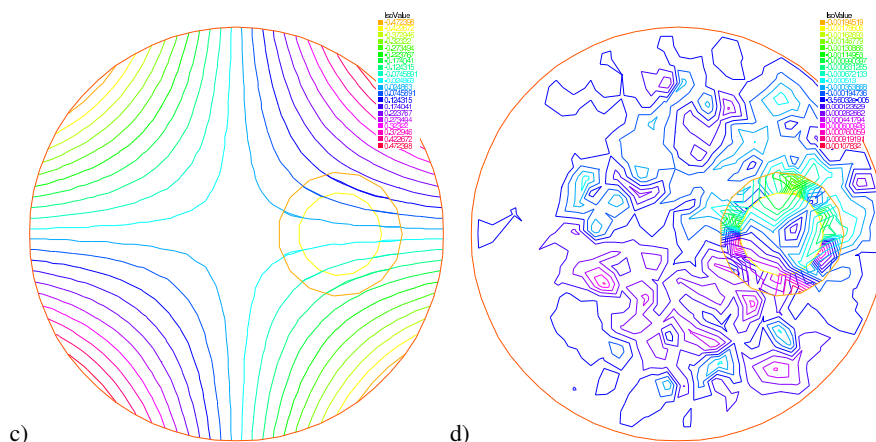


**Fig. 3.** c) The solution obtained by the Schwarz algorithm on M1; d) The error with respect to the exact continuous solution.

### 3 Numerical Comparison of the Methods

We tested all the Algorithms 2-4 on the benchmark of the Poisson equation  $-\Delta u = f$  in  $\Omega = (-1, 1)^2$  with Dirichlet boundary conditions on  $\partial\Omega$  and the exact solution

$$u = \cos \frac{\pi}{2}x \cos \frac{\pi}{2}y + 10\chi(x^2 + y^2 < R^2)e^{\frac{1}{R^2} - \frac{1}{R^2 - x^2 - y^2}} \quad (30)$$

with  $R = 0.3$ . We choose the patches of the form  $\Lambda = (-\varepsilon_\Lambda, \varepsilon_\Lambda)^2$ , the holes in  $\Omega$  of the form  $D = (-\varepsilon_D, \varepsilon_D)^2$  and take the triangulations  $\mathcal{T}_H$  and  $\mathcal{T}_h$  that do not match each other, but the hole  $D$  always consists of several triangles from  $\mathcal{T}_H$ . We used the following options to compute the mixed integrals in (5)-(6) (the same holds for (8)-(10)): the integral  $\int_\Omega \nabla u_h^{n-1} \cdot \nabla w_H$  in (5) is evaluated by a numerical quadrature on the fine mesh  $\mathcal{T}_h$ , the integral  $\int_\Lambda \nabla u_H^n \cdot \nabla w_h$  in (6) is approximated by  $\int_\Lambda \nabla(\gamma_h u_H^n) \cdot \nabla w_h$ , which is easy to evaluate.

Figure 4 presents the convergence history in the  $H^1$  and  $L^\infty$  norms of the relative error on iterations for the 4 choices of triangulations. We observe that all the methods converge but that the Harmonic Patch Iterator is in general the most efficient approach. More specifically, it converges to a better approximation in situations a) and b) with the patch of the size  $\varepsilon_\Lambda = 0.27$ . The gain in accuracy is observed in both  $H^1$  and  $L^\infty$  norms. On the contrary, all the methods converge to virtually the same approximated solution in situations c) and d) where we have taken a larger patch with  $\varepsilon_\Lambda = 0.4$ . However, this choice of meshes does not allow us to compare the relative merits of our algorithms. Indeed, the patch here is so large that the solution outside  $\lambda$  does not feel the spike in  $f$ , which lies inside  $\Lambda$ . Therefore, one does not need to iterate here at all: one coarse calculation with one fine correction gives already a fairly good solution. Note also that the errors in Fig. 4 are computed with respect to the exact solution so that these results confirm the convergence of all the methods under mesh refinement.

We do not give here detailed results on our last Algorithm 5 since these results are very close to those of Algorithm 4 for the present benchmark.

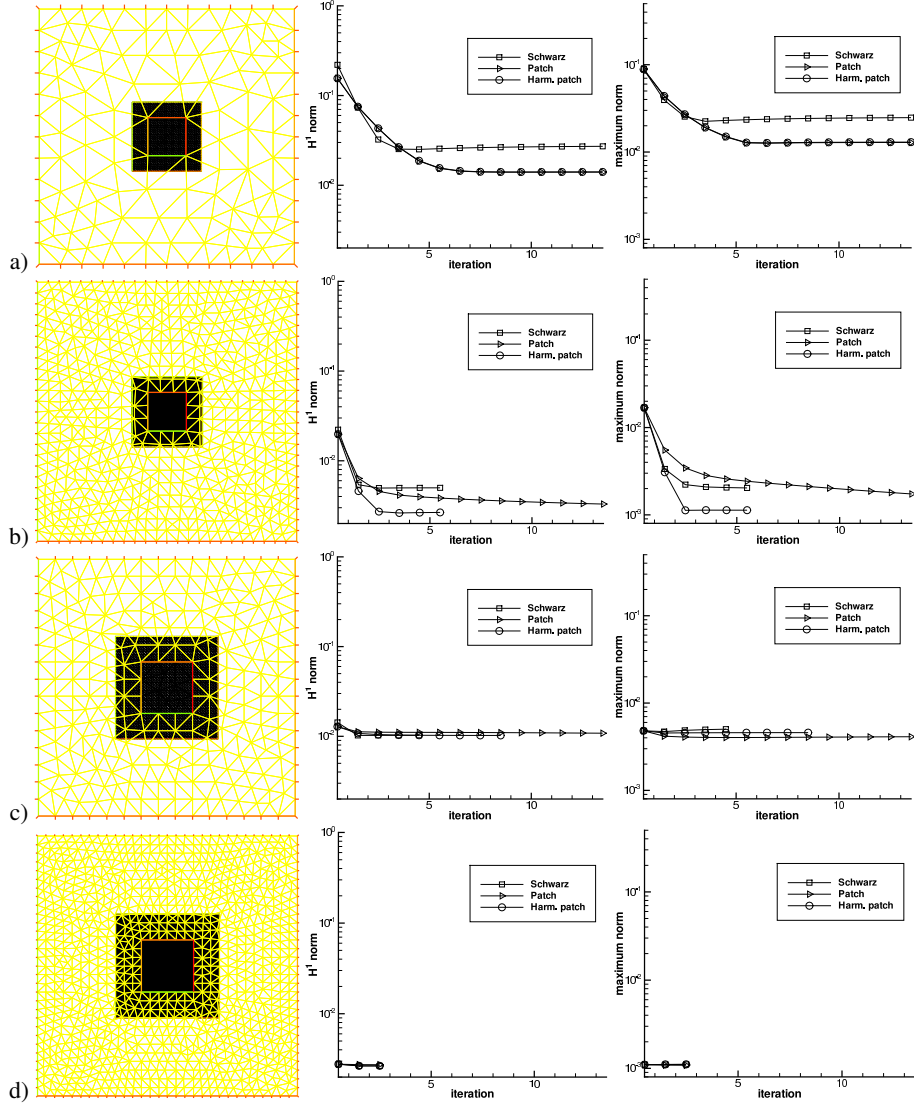


**Fig. 4.** Results for the benchmark (30). Left – the meshes, middle – relative error on iteration in the  $H^1$  norm, right – relative error in the  $L^\infty$  norm. Four pairs of meshes: a)  $\varepsilon_A = 0.27$ ,  $\varepsilon_D = 0.15$ ,  $H = \frac{1}{6}$ ,  $h = \frac{0.27}{15}$ ; b) the twofold refinement of a); c)  $\varepsilon_A = 0.4$ ,  $\varepsilon_D = 0.2$ ,  $H = \frac{2}{15}$ ,  $h = \frac{1}{50}$ ; d) the twofold refinement of c).

## 4 Conclusion

The paper has shown that a standard Schwarz algorithm can be used for a zooming procedure, even with standard interpolations at the boundaries. However it seems that if one needs to iterate between the coarse and fine scales, the Harmonic Patch approach is the most robust way to do it. The numerical quadrature could affect the subspace correction methods in some cases. In order to get rid of the quadrature, one can compute the mixed integrals exactly on the intersection of two triangulations. In the near future we plan to improve on our triangulation intersector by inserting Martin Gander et al 's algorithm [6] into freefem++.

## References

- [1] Achdou, Y., Maday, Y.: The mortar element method with overlapping subdomains. *SIAM J. Numer. Anal.*, 40(2):601–628, 2002.
- [2] Apoung Kamga, J.-B., Pironneau, O.: Numerical zoom for multiscale problems with an application to nuclear waste disposal. *J. Comput. Phys.*, 224(1):403–413, 2007.
- [3] Brezzi, F., Lions, J.-L., Pironneau, O.: Analysis of a Chimera method. *C. R. Acad. Sci. Paris Sér. I Math.*, 332(7):655–660, 2001.
- [4] Cai, X.-C., Mathew, T.P., Sarkis, M.V.: Maximum norm analysis of overlapping nonmatching grid discretizations of elliptic equations. *SIAM J. Numer. Anal.*, 37(5):1709–1728 (electronic), 2000.
- [5] Ciarlet, P.G., Raviart, P.-A.: Maximum principle and uniform convergence for the finite element method. *Comput. Methods Appl. Mech. Engrg.*, 2:17–31, 1973.
- [6] Gander, M.J., Japhet, C.: A compact algorithm with optimal complexity for non-matching grid projections. In *Proceedings of the 18th international conference of Domain Decomposition methods*, (these proceedings).
- [7] Glowinski, R., He, J., Lozinski, A., Rappaz, J., Wagner, J.: Finite element approximation of multi-scale elliptic problems using patches of elements. *Numer. Math.*, 101(4):663–687, 2005.
- [8] He, J., Lozinski, A., Rappaz, J.: Accelerating the method of finite element patches using approximately harmonic functions. *C. R. Math. Acad. Sci. Paris*, 345(2):107–112, 2007.
- [9] Hecht, F., Lozinski, A., Perronnet, A., Pironneau, O.: Numerical zoom for multiscale problems with an application to flows through porous media. *Disc. Cont. Dyna. Syst.*, submitted, 2007.
- [10] Hecht, F., Pironneau, O., Le Hyaric, A., Ohtsuka, K.: Freefem++, ver. 2.23. <http://www.freefem.org>, 2007.
- [11] Dougherty, F.C., Steger, J.L., Benek, J.A.: A Chimera grid scheme. In *Advances in Grid Generation*. K.N. Chis and U. Ghia eds., ASME FED-vol. 5. June 1983.
- [12] Liions, J.-L., Pironneau, O.: Domain decomposition methods for CAD. *C. R. Acad. Sci. Paris Sér. I Math.*, 328(1):73–80, 1999.
- [13] Schatz, A.H., Wahlbin, L.B.: On the quasi-optimality in  $L_\infty$  of the  $\dot{H}^1$ -projection into finite element spaces. *Math. Comp.*, 38(157):1–22, 1982.